Analysis of NEACRP 3D BWR Core Transient Benchmark

Vyacheslav G. Zimin, Hideaki Asaka, Yoshinari Anoda
Department of Reactor Safety Research
Japan Atomic Energy Research Institute
Tokai-mura, Ibaraki-ken, 319-1195, Japan,
Tel.: +81-29-282-5357;
Fax: +81-29-282-6728;
E-mail: slava@lstf3.tokai.jaeri.go.jp

Elja Kaloinen, Riitta Kyrki-Rajamäki
VTT ENERGY / Nuclear Energy
P.O. Box 1604
FIN-02044 VTT, Finland
Tel: +358-9-456-5014
Fax: +358-9-456-5000
E-mail: Elja.Kaloinen@vtt.fi

Abstract

NEACRP BWR cold water injection benchmark is analyzed by two codes: TRAC-BF1/SKETCH-N code system by JAERI, Japan and TRAB-3D code by VTT Energy, Finland. Basic features of the codes are described. Neutronics modules of the codes apply nodal methods; separate calculations are performed to compare their accuracy. Thermal-hydraulics modules are significantly different: TRAC-BF1 uses two-phase two-fluid model, while TRAB-3D applies drift-flux model with four separated equations. A representative set of the global and local reactor parameters is given for both the steady-state and transient conditions. TRAB-3D calculations have been performed with two slip correlations: EPRI and the simple Zuber-Findley correlation. A comparison of the two TRAB results shows the importance of the slip model on some computed reactor parameters. The results of the TRAC-BF1/SKETCH-N and TRAB-3D codes are in a close agreement, especially when the advanced EPRI correlation is used in the TRAB-3D code. The presented data can be useful for assessment of other BWR codes.

1 Introduction

International benchmark problems have proved to be valuable tools for assessment of the coupled neutronics/thermal-hydraulics reactor analysis codes. Useful experience has been gained by many code developers participating in PWR rod ejection and rod withdrawal benchmarks, conducted by Reactor Physics Committee (NEACRP) of the OECD Nuclear Energy Agency. 3D light water reactor (LWR) core transient benchmarks (Finnemann and Galati, 1992) include two problems for boiling water reactor (BWR) cores: case D1 – cold water injection and case E1 – overpressurization transient. The final benchmark report provides case D1 results presented by eight national and industrial institutions from five countries (Finnemann et al., 1993). However, only a few reactor parameters are given and discrepancies between the results are large. For example, the reactor multiplication factors differ by 600 pcm (1 pcm = 0.001 %) and the reactor power peaks in the transient differ by 200 %. It is difficult to make a comparison with these results. Probably due to these reasons NEACRP BWR benchmarks has not gained such popularity as similar PWR or VVER exercises.

The paper presents the results of the NEACRP BWR cold water injection benchmark computed by two codes: TRAC-BF1/SKETCH-N code system developed in JAERI and TRAB-3D developed in VTT Energy of Finland. The calculations are performed as a part of verification of both the codes. The presented results, which are in a close agreement, can also be used for assessment of other BWR computer programs. The paper is organized as follows. Section 2 of the paper gives overview of the TRAC-BF1/SKETCH-N code system. The basic features of the neutron kinetics code SKETCH-N are given in Section 2.1, TRAC-BF1 code is described in Section 2.2. An interface module developed for a coupling of the codes is discussed in Section 2.3. Section 3 outlines the main features of the BWR transient analysis code TRAB-3D. Section 4 starts with description of the BWR cold water benchmark. The reactor model used in the TRAC-BF1/SKETCH-N calculations is given in Section 4.2, Section 4.3 shows the model used in the TRAB-3D code. Section 5 presents the numerical results of both the steady-state and transient calculations. The TRAB-3D results are computed with the slip correlation developed in EPRI and as a sensitivity study also with the simple Zuber-Findley correlation. A comparison between two TRAB results outlines effect of the accurate modelling of the differing velocities of the vapor and liquid phases on several reactor parameters. Neutronics modules of the codes are compared considering the results of the steady-state calculations performed with the same set of the thermal-hydraulics feedbacks. The results are very close to each other in this case demonstrating that the discrepancies in the benchmark results are mostly due to the thermal-hydraulics (or neutron kinetics) models. A comparison between the TRAC-BF1/SKETCH-N and TRAB-3D results shows reasonable agreement, especially in the case when the slip correlation of EPRI is used in the TRAB-3D code. Conclusions of the paper are given in Section 6.

2 TRAC-BF1/SKETCH-N Code System

TRAC-BF1/SKETCH-N code system has been recently developed in JAERI by a coupling of the transient analysis code TRAC-BF1.MOD1 with the three-dimensional neutron kinetics code SKETCH-N. The both codes are written in FORTRAN 77; the coupling interface module is based on the message-passing library PVM (Parallel Virtual Machine). The code system includes a preprocessor to generate the TRAC input deck for the case when a number of thermal-hydraulics channels is an order of hundreds. Postprocessing capabilities include 1D graphics utilities GCONV/IPLOT and 2D/3D graphics PLOT-ACE.

2.1 TRAC-BF1 code

TRAC-BF1 is a version of the TRAC code modified in Idaho National Engineering Laboratory (INEL) for BWR analysis (Borkowski et al., 1992). A hydrodynamics model of the code is a two-phase two-fluid model with explicit flow regime maps. Six conservation equations for mass, energy and momentum are formulated for vapor and liquid phases for one-dimensional flow. A reactor vessel can be described in three-dimensional cylindrical coordinates. TRAC has a flow-regime-dependent constitutive equation package, providing a large number of closure relations for interfacial area, interfacial mass transfer rate, interfacial drag coefficients, liquid wall-drag coefficient etc. Fuel rod heat conduction module solves 1D(radial) or 2D(R-Z) heat conduction equations. Heat transfer at the outer cladding surface is modeled separately to liquid and gas phases. A boiling curve is subdivided into single-phase liquid, nucleate boiling, transition boiling, film boiling, single-phase vapor and condensation modes. A constant value is used for the gap heat conductivity. Semi-implicit stability enhanced two-step (SETS) method is applied in time discretization of the fluid flow equations. Standard finite-different methods are used for space discretization of the both fluid flow and heat conduction equations; the heat conduction axial mesh is staggered with respect to the fluid dynamics axial mesh. TRAC-BF1 component library has traditional components of the TRAC codes and several specific BWR modules: `CHANNEL`, `JET PUMP`, `SEPARATOR-DRYER`, and `FEEDWATER HEATER`.

Neutron kinetics modules include point kinetics and 1D models. These models significantly limit the best-estimate capabilities of the code for many BWR transients. To remove this limitation the 3D neutron kinetics code SKETCH-N has been coupled with the TRAC-BF1 code.

2.2 SKETCH-N code

The SKETCH-N code (Zimin and Ninokata, 1998; Zimin, 2000) solves neutron diffusion equations in Cartesian geometry for steady-state and kinetics problems. The code can treat an arbitrary number of neutron energy groups and delayed neutron precursors. Polynomial, semi-analytic and analytic nodal methods based on the nonlinear iteration procedure can be used for spatial discretization of diffusion equations (Zimin et al., 1998). Time integration of the neutron kinetics equations is performed by the fully-implicit scheme with an analytical treatment of the delayed neutron precursors. Steady-state eigenvalue problems are solved by inverse iterations with a Wielandt shift accelerated by Chebyshev polynomials. An adaptive Chebyshev iterative procedure is used for neutron kinetics problems. The block symmetric Gauss-Seidel method is applied as a preconditioner in both the steady-state and transient problems. An automatic time step control based on the time step doubling technique is used in the code.

An extensive set of the steady-state and neutron kinetics LWR benchmarks has been calculated to verify the SKETCH-N code (Zimin et al., 1998; Zimin and Ninokata, 1998). The results show that the SKETCH-N code has acceptable accuracy and efficiency to be used in the LWR safety analysis and design. The code has been also coupled with the J-TRAC (TRAC-PF1) code (Akimoto et al., 1989), the J-TRAC/SKETCH-N code system has been verified against NEACRP PWR rod ejection and rod withdrawal benchmarks (Zimin et al., 1999; Asaka et al., 2000).

2.3 Coupling Interface Module

A coupling of the SKETCH-N code with the TRAC-BF1 code is performed using an interface module. The codes are treated as separate processes, and the interface module is responsible for data exchange between the codes, data mapping between the spatial meshes of the codes and synchronization of time stepping. The interface module is based on the message-passing library PVM (Geist et al., 1994). The TRAC and SKETCH-N codes usually perform calculations using different spatial meshes, thus requiring a mapping of the data between the neutronics, heat conduction and fluid dynamics meshes. The mapping procedure based on the mapping matrix approach has been developed. For each pair of the spatial meshes a code user define two mapping matrices: a mapping matrix describing a correspondence of the 2D radial meshes and a mapping matrix for 1D axial meshes. The interface module transfers power distribution from SKETCH into the TRAC code, Doppler fuel temperatures and coolant densities (void) are transferred in the opposite direction. The programs also exchange the values of time step size. Detailed description of the interface module is given in (Zimin et al., 1999; Asaka et al., 2000; Zimin, 2000).

3 TRAB-3D Code

TRAB-3D that is entirely developed in Finland, is a three-dimensional reactor dynamics code for transient and accident analyses of BWR and PWR reactors (Kaloinen et al., 1998, Kaloinen and Kyrki-Rajamäki 1997). The development of dynamics codes has continued some 25 years at VTT Energy and TRAB-3D is a direct descendant of the 1D code TRAB (Rajamäki, 1980) and the 3D hexagonal code HEXTRAN (Kyrki-Rajamäki, 1991). In TRAB-3D, the neutron kinetic model is similar to HEXTRAN, but calculation models for the thermal hydraulics in core and primary circuit of a BWR are adopted from TRAB.

3.1 Neutronics model

The two-group neutron diffusion equations are solved in TRAB-3D by a nodal expansion method in x-y-z geometry within the reactor core (Kaloinen and Kyrki-Rajamäki, 1997). The solution method is an adaptation to Cartesian geometry of the hexagonal method that was originally developed for the fuel management code HEXBU-3D (Kaloinen, et al., 1979) and later applied in HEXTRAN. A basic feature of the method is decoupling of the two-group equations into separate equations for two spatial modes and construction of group fluxes from characteristic solutions to these equations. The two solutions are called fundamental or asymptotic mode which have a fairly smooth behavior within a homogenized node, and transient mode which have a large and negative buckling in LWR reactors. The transient mode deviates significantly from zero only near material discontinuities. The fundamental mode of flux is assumed separable in radial and axial directions within a node and both components are approximated by a high order polynomial. Due to different behavior, the transient mode is approximated by exponential functions at each face of the node. Altogether, the flux model contains 20 degrees of freedom or unknown parameters per node. The parameters, or rather the coupling coefficients of adjacent nodes, are determined by an equal number of relations which are given by continuity conditions of average flux and net current and of their first moments at nodal interfaces. In radial direction, the flux can be discontinuous between nodes if flux discontinuity factors are included in input data.

The nodal equations are solved with a two-level iteration scheme where only one unknown per node, the average of fundamental mode, is determined in inner iterations. The nodal flux shapes are improved in outer iterations by recalculation of the coupling coefficients. A thermal-hydraulic calculation is also performed during these iterations and the nodal cross sections are updated for current conditions of the reactor core. Cross sections are computed from polynomial fittings to fuel and coolant temperature, coolant density and soluble boron density.

The solution method is applied for the homogeneous eigenvalue equation of steady state as well as for the inhomogeneous time discretized equations of neutron kinetics. To ensure the initial criticality of the reactor, the fission production cross sections are divided by k-effective after the steady state calculation. The time discretization is made by implicit methods that allow a flexible choice of time steps. Automatic time step choice can be used. During a time step the flux is assumed separable in space and time variables and the delayed neutron source has the same distribution as the source of prompt fission neutrons within a node. At most six delayed neutron groups is used in TRAB-3D.

3.2 Thermal-hydraulics

Thermal-hydraulic calculation of the reactor core is performed in parallel hydraulic channels that are usually coupled with one fuel assembly each. A core bypass channel and unheated channel regions at inlet and outlet of the core may be included in the calculation model. Channel hydraulics is based on conservation equations for steam and water mass, total enthalpy and total momentum, and on a selection of optional correlations describing e.g. non-equilibrium evaporation and condensation, slip, and one and two-phase friction. Distribution of coolant flow through the channels is determined by pressure balance over the core and the phase velocities are related by an algebraic slip ratio or by the drift flux formalism. Water and steam properties are calculated from rational functions of pressure and enthalpy. Hydraulic equations are solved in a one-dimensional axial geometry within the channels, which is an accurate method for reactors with shroud tubes around fuel assemblies.

During hydraulic iterations a one-dimensional heat transfer calculation with several radial mesh points is made for an average fuel rod at different axial elevations in each hydraulic channel. Thermal properties of fuel pellet, gas gap and fuel cladding are functions of burnup and temperature and the heat transfer coefficient depends on the hydraulic regime. The fission power is divided into prompt and delayed fractions (decay power) and part of the power can be dissipated into heat directly in the coolant.

Advanced time integration methods are applied in the dynamic calculation. The numerical technique can vary between the standard fully implicit theta method and the central-difference theta method both in the heat transfer calculation for fuel rods and in the solution of thermal-hydraulic conservation equations for cooling channels.

TRAB-3D includes the BWR circuit model containing one-dimensional descriptions for the main circulation system inside the reactor vessel including the steam dome with related systems, steam lines, recirculation pumps, incoming and outgoing flows and control and protection systems. A four-quadrant homologous pump model is used for description of the recirculation pumps and there is a possibility to describe several pump groups with different qualities. Effects of superheated or wetted steam are considered in the model for the steam dome and the steam lines. Since the benchmark problem is a core transient, the circuit model is not used in the calculations, but the reactor pressure and total coolant flow are kept constant during the transient.

TRAB-3D has also been coupled with the thermal hydraulics code SMABRE developed in VTT which can be used for modelling of PWR, BWR or VVER circuits. The PWR model has recently been validated with the OECD NEA Main Steam Line Break benchmark.

4 NEACRP BWR Cold Water Injection Benchmark

NEACRP BWR cold water injection benchmark is the case D1 of the LWR 3D core transient benchmarks proposed by H. Finnemann and A. Galati (1992). The reactor core consists of 185 fuel and 64 reflector macroelements; each represents four regular subassemblies homogenized with a control blade. An introduction of macroelements simplifies actual BWR core configuration reducing the number of nodes in the X-Y plane by a factor of four. Each macroelement is subdivided into 14 axial layers of 30.48 cm height. 10 types of macroelements are defined, 19 material compositions are used to describe the macro cross sections. Two prompt neutron energy groups and six groups of delayed neutron precursors are considered. The macro cross sections are given as polynomial functions of the coolant density and Doppler fuel temperature. The problem has detail description of material properties of fuel rods, including temperature dependencies of the heat conductivity and the heat capacity of fuel and cladding. Gap conductance constant is also given. The macroelements are subdivided into two types with respect to inlet orifice diameter. Inlet pressure drop is defined as

$$\Delta P = c\, G^2 , \tag{1}$$

where

ΔP is the inlet pressure drop (*bar*);

$c = 2.23\times10^{-4}$ for standard macroelement and $c = 3.79\times10^{-4}$ for peripheral macroelement;

G is the macroelement mass flow rate (*kg/s*).

Frictional pressure drop inside a channel is given as

$$\partial p \big/ \partial z = 2.\times10^{-6} G^2 f(x) ,$$

where

$\partial p \big/ \partial z$ is the frictional pressure gradient (*bar/cm*);

G is the bundle mass flow rate (*kg/s*);

x is the steam quality;

$f(x)$ is the frictional factor given in the Table 5.25 of the benchmark specification.

Please note that in the expression for frictional pressure drop, G is the bundle mass flow rate, not the macroelement mass flow rate as stated in the benchmark specification. This misprint is explained by E. Sartori in the letter to benchmark participants (1992).

Cold water injection over the whole core is simulated by doubling the inlet water subcooling through an exponential increase with 2.5 s time constant as follows

$$\Delta H = 46.52\left(2 - \exp[-0.4\, t] \right),$$

where

ΔH is the inlet subcooling enthalpy (*kJ/kg*);

t is time (*s*).

4.1 TRAC-BF1/SKETCH Benchmark Model

Neutronics model of the benchmark has been developed for the SKETCH-N code based on the benchmark specification without any simplifications. The polynomial macro cross section model is implemented into the code. The SKETCH-N calculations are performed using a spatial mesh 17x17x26 with 1 node per macroelement and 26 axial layers: top and bottom axial reflector layers are 30.48 cm height and 24 layers in the reactor core of 15.24 cm height. An automatic time step control procedure has been used. Criticality of the initial condition is set by dividing an average number of neutrons per fission by a steady-state multiplication factor.

The TRAC-BF1 reactor model is illustrated in Fig. 1. The `VESSEL` component with 185 `CHANNEL`s is used to simulate the reactor core. Channel's axial mesh has 24 layers, which coincides with the neutronics axial mesh in the reactor core. The reactor boundary conditions are given using a `FILL` component on the bottom, which defines inlet coolant properties and a `BREAK` component on the top, which specifies the reactor pressure of 6.7 MPa. A radial heat conduction mesh in fuel rods has 6 zones in the fuel and 2 zones in the cladding. The fuel rod material properties defined in the benchmark are implemented as an option in the TRAC-BF1 code. The frictional pressure drop in the channels is also directly coded. The inlet pressure drop in the TRAC is defined as

$$\Delta P = \frac{1}{2} K \rho \mathrm{v}^2 , \qquad (2)$$

where

ΔP is inlet pressure drop (*Pa*);
K is the TRAC input constant;
ρ is coolant density (kg/m^3);
v is the coolant velocity (*m/s*).

Using Eq. (1)-(2) and converting into the SI units we get

$$K = 2 \times 10^5 \rho A^2 c ,$$

where

A is the macroelement flow area (m^2).

Applying $A = 4.0078 \times 10^{-2}\ m^2$ and $\rho = 763.1\ kg/m^3$ we obtain the TRAC input constants as $K = 57.12$ for standard macroelements and $K = 92.91$ for peripheral macroelements.

The inlet cold water injection is simulated as the tables of the FILL component by defining the inlet coolant temperature, velocity and pressure.

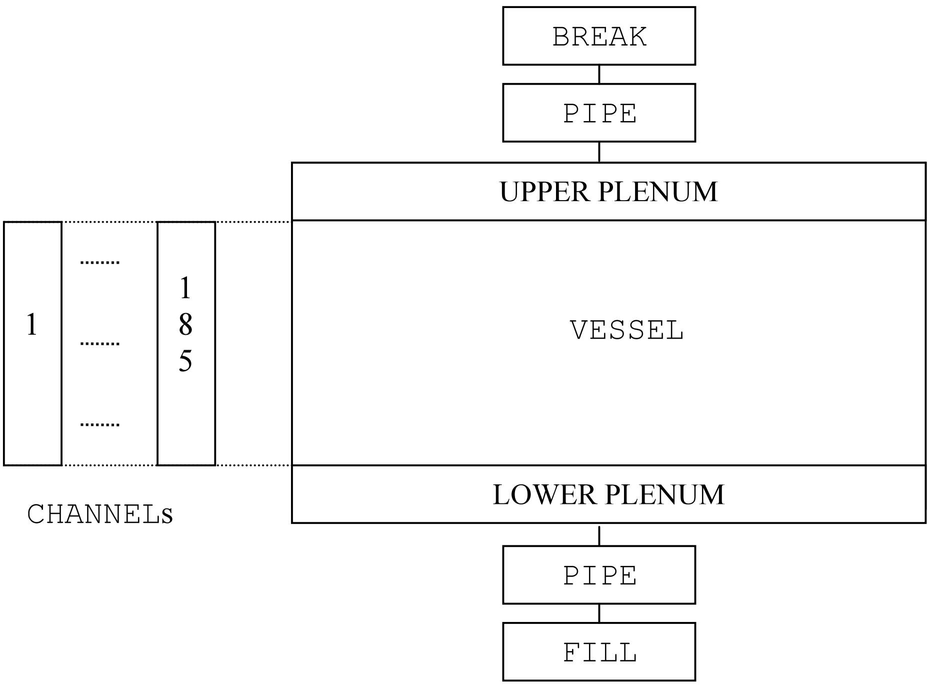

Figure 1. TRAC-BF1 model of the BWR cold water injection benchmark.

4.2 TRAB-3D Benchmark Model

In TRAB-3D model, only the reactor core is included in the neutronic calculation and the reflectors are replaced by albedo boundary conditions. The polynomial approximation of intranodal flux in TRAB-3D does not work well in reflectors where flux gradient tends to be large. In a transverse cross section, the core consists of 185 nodes or one node per macroelement and axially the core is divided into 24 nodes of equal height. The two-group albedos of axial reflectors are derived from the known relation between cross sections and albedos for a plane reflector of infinite thickness. Since the relation is less accurate for radial reflectors the standard albedos for ABB type BWR reactors are used in the benchmark calculation. The adequacy of the albedos can be estimated by comparison of power distributions with SKETCH-N in Fig. 2. The agreement is excellent, though somewhat higher relative deviations appear in some peripheral elements. However, due to very low power of these elements, the significance of the deviations in transient calculation is negligible.

Some minor approximations are made for the cross section data in the calculation. In TRAB-3D, the diffusion coefficient, not the transport cross section, depends on fuel Doppler temperature and this requires a modification of the derivative terms to operate on diffusion coefficients. Other approximations concern fission cross sections. Because in TRAB-3D the number of fission neutrons cannot depend on fuel temperature or water density, the fission cross sections are calculated from the current values of fission production cross sections ($\nu\Sigma_f$) by division with the nominal value of fission neutrons. Thus the separate feedback coefficients for fission cross sections are not used in the calculation.

The thermal-hydraulic calculation uses the same nodal division in the core as the neutronic calculation. Each macroelement is represented with a separate hydraulic channel in which a one-dimensional calculation is performed. The different inlet throttling of coolant flow is described by individual values of local friction coefficient in the unheated lower region of the channels and the frictional pressure loss is treated according to the problem formulation. Heat transfer from fuel cladding to coolant is calculated with Dittus-Boelter correlation for forced convection and from Thom´s correlation for nucleate boiling. Evaporation/condensation model is a nonequilibrium model of RAMONA (Holt and Rasmussen, 1972). Two alternatives for the slip model are applied: the drift flux model of EPRI (Chexal and Lellouche, 1986) and for comparison the Zuber-Findley model (Zuber et al., 1967). The latter model is rather simple and is not accurate but within a restricted range of hydraulic conditions. The EPRI model is more complicated and covers a large range of conditions.

Distribution of coolant flow through hydraulic channels is determined by pressure balance over the core and the total flow is kept constant during the transient calculation. At steady state the core pressure loss is 0.2285 MPa when the EPRI correlation is used. Heat transfer equations are solved for an average fuel rod in each hydraulic (or neutronic) node. The solution uses a radial mesh of 7 points in fuel pellet and 2 points in cladding. The Doppler temperature is calculated according to the problem specification that differs slightly from the original definition of the temperature in TRAB-3D.

The time steps are predetermined in input of the calculation and their lengths vary within 5-50 ms during the transient. The minimum length of 5 ms is applied for transient time 0.8-2.8 s around the power maximum where the temporal change of reactor conditions is fastest. A test calculation showed that a further decrease of the step length has a negligible effect on the results.

5 Numerical Results

The benchmark problem report gives the results of eight industrial and national institutions from five countries (Finnemann et al., 1993). The discrepancies between the published results are large: about 600 pcm for the steady-state eigenvalue, and almost 200 % in the power peak. In the following, we decided not to present a comparison with the published results, but to compare only the TRAC-BF1/SKETCH-N and TRAB-3D data. A comparison is performed against the TRAC-BF1/SKETCH-N results. It does not mean that the TRAC-BF1/SKETCH-N code system is more accurate than the TRAB-3D code, it is simply a matter of agreement to present the data.

5.1 A Comparison of the Neutronics Modules

To exclude an influence of thermal-hydraulics feedbacks we compared the results of the steady-state calculations with the same set of the thermal-hydraulics feedbacks generated by the TRAB-3D code with Zuber-Findley correlation. The SKETCH-N calculations are performed using two spatial meshes: the mesh 17x17x26, which is used in the benchmark analysis, and the mesh 34x34x52 with a half mesh size. The two SKETCH-N calculations are in excellent agreement, the maximum difference in 2D power distribution is 1.4 % and the differences in 1D power distribution are below 1 %. The TRAB-3D code applied the mesh 15x15x24, where the radial and axial reflectors are treated as albedo boundary conditions. A summary of the SKETCH-N and TRAB-3D results is given in Table 1, where a comparison is performed with respect to the SKETCH-N results on the mesh 17x17x26. The differences in the power peaking factors are below 2 %, the maximum difference in the reactor multiplication factors is 52 pcm. 2D power distributions computed by the SKETCH-N and TRAB-3D codes are slightly different as shown in Fig. 2. The reactor core is almost symmetric; only the quarter-core results are given. The maximum differences in 2D power distribution are in the peripheral macroelements; they are mostly due to an application of the albedo boundary conditions in the TRAB-3D code. The power of the peripheral channels is very low, so these differences are not significant. The results show that both the SKETCH-N and TRAB-3D codes provide accurate results on the selected spatial meshes.

Table 1. A comparison of pure neutronics modules for the steady-state calculations of the NEACRP BWR cold water benchmark. TRAB-3D (Zuber-Findley correlation) results and SKETCH-N results computed with TRAB-3D feedbacks.

Parameter	SKETCH-N mesh 17x17x26	SKETCH-N mesh 34x34x52	TRAB-3D mesh 15x15x24
Eigenvalue	0.98582	0.98597 *+15 pcm*	0.98634 *+52 pcm*
1D axial power peaking factor	1.359	1.364 *+0.4 %*	1.347 *-0.9 %*
2D radial power peaking factor	2.017	2.012 *-0.2 %*	2.002 *-0.7 %*
3D power peaking factor	3.118	3.117 *-0.03 %*	3.066 *-1.7 %*

TRAB-3D (Zuber-Findley correlation)
SKETCH-N (TRAB-3D feedbacks)
DIF(%)

	1	2	3	4	5	6	7	8
1:					0.054	0.084	0.108	0.140
1:					0.056	0.086	0.108	0.140
1:					-4.3	-1.8	0.0	-0.1
2:				0.121	0.284	0.418	0.450	0.628
2:				0.121	0.285	0.415	0.451	0.614
2:				0.5	-0.3	0.8	-0.2	2.3
3:			0.138	0.402	0.982	1.207	1.224	1.174
3:			0.139	0.406	0.977	1.202	1.222	1.169
3:			-0.6	-0.8	0.6	0.4	0.2	0.5
4:		0.124	0.413	1.024	1.509	1.565	1.577	1.142
4:		0.124	0.416	1.020	1.509	1.566	1.570	1.144
4:		0.6	-0.8	0.4	0.0	0.0	0.4	-0.2
5:	0.060	0.287	0.987	1.512	1.755	1.735	1.844	1.789
5:	0.062	0.288	0.982	1.511	1.762	1.732	1.853	1.787
5:	-3.7	-0.3	0.5	0.0	-0.4	0.2	-0.5	0.1
6:	0.093	0.421	1.210	1.567	1.736	1.327	1.868	1.876
6:	0.094	0.418	1.205	1.568	1.732	1.332	1.869	1.883
6:	-1.5	0.7	0.4	0.0	0.2	-0.3	-0.1	-0.4
7:	0.120	0.454	1.227	1.578	1.844	1.868	2.002	1.954
7:	0.119	0.455	1.224	1.571	1.854	1.870	2.017	1.957
7:	0.2	-0.2	0.2	0.4	-0.5	-0.1	-0.7	-0.2
8:	0.153	0.632	1.177	1.143	1.789	1.876	1.954	1.513
8:	0.153	0.618	1.171	1.145	1.788	1.883	1.957	1.518
8:	0.1	2.3	0.5	-0.2	0.1	-0.4	-0.2	-0.3

Max. difference in 2D power distribution: -4.28 %; Location (x,y): (5,1)
Average difference in 2D power distribution: 0.60 %
2D Power Peaking Factor (SKETCH-N): 2.0170 Location (x,y):(7,7)
2D Power Peaking Factor (TRAB-3D) : 2.0023 Location (x,y):(7,7)
Difference in 2D Power Peaking Factors: -0.73%

Figure 2. A comparison of 2D power distributions computed by the SKETCH-N code (mesh 17x17x26, computed with TRAB-3D feedbacks) and by the TRAB-3D code (mesh 15x15x24, Zuber-Findley correlation).

5.2 Steady-State Results

A summary of the steady-state results is given in Table 2. There is a close agreement between the TRAC-BF1/SKETCH-N and TRAB-3D results, especially in the case when TRAB-3D code applies the EPRI correlation. The core-averaged axial power distribution is shown in Fig. 3. Axial distribution of the coolant density is given in Fig. 4. A choice of the slip correlation has significant effect on the axial void distribution and consequently on the axial profiles of the coolant density and power. The mass flow rates and the outlet coolant densities along the vertical traverse are shown in Fig. 5 and 6. Mass flow rate is not sensitive to the choice of the slip correlation, because the frictional pressure drop depends only on steam quality. The outlet coolant density changes by 4 % when slip correlation is changed in TRAB-3D. Radial power density is not very sensitive to the slip correlation. In Fig. 7, 2D power distributions of the TRAC-BF1/SKETCH-N code system and TRAB-3D code with EPRI correlation are compared. The agreement is good; the differences are mostly due to the use of albedo boundary conditions in the TRAB-3D code as shown in Section 5.1.

Table 2. Summary of the TRAC-BF1/SKETCH-N and TRAB-3D steady-state results of the NEACRP BWR cold water injection benchmark.

Parameter	TRAC-BF1/ SKETCH-N	TRAB-3D EPRI Slip Correlation	TRAB-3D Zuber-Findlay Correlation
Eigenvalue	0.98439	0.98312 *-127 pcm*	0.98634 *+195 pcm*
1D axial power peaking factor	1.444	1.391 *-3.7 %*	1.347 *-6.7 %*
2D radial power peaking factor	1.955	1.983 *+1.4 %*	2.002 *+2.4 %*
3D power peaking factor	3.312	3.198 *-3.4 %*	3.066 *-7.4 %*
Core-averaged Doppler fuel temperature, (°C)	499	512 *+13 °C*	511 *+12 °C*
Maximum Doppler fuel temperature, (°C)	1105	1119 *+14 °C*	1077 *-28 °C*
Maximum centerline fuel temperature, (°C)	2112	2086 *-26 °C*	1987 *-125 °C*
Outlet coolant temperature, (°C)	282.1	282.1 -	282.1 -
Outlet coolant density, (kg/m^3)	452.7	444.6 *-8.1 kg/m^3*	456.0 *+3.3 kg/m^3*
Outlet void fraction	0.426	0.425 *-0.001*	0.409 *-0.017*

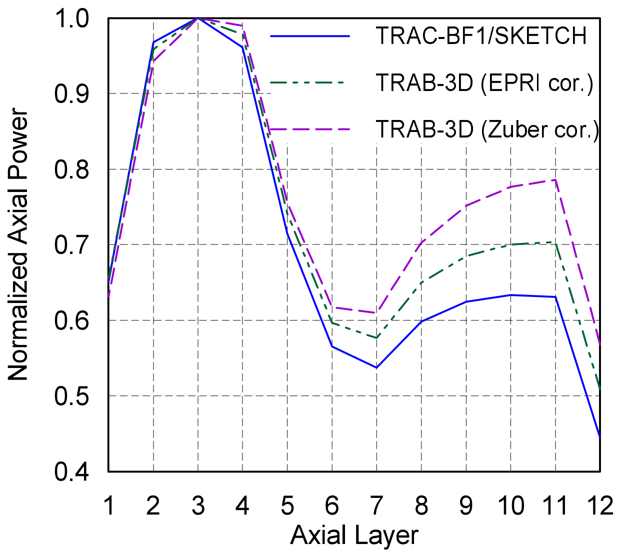

Figure 3. Normalized axial power.

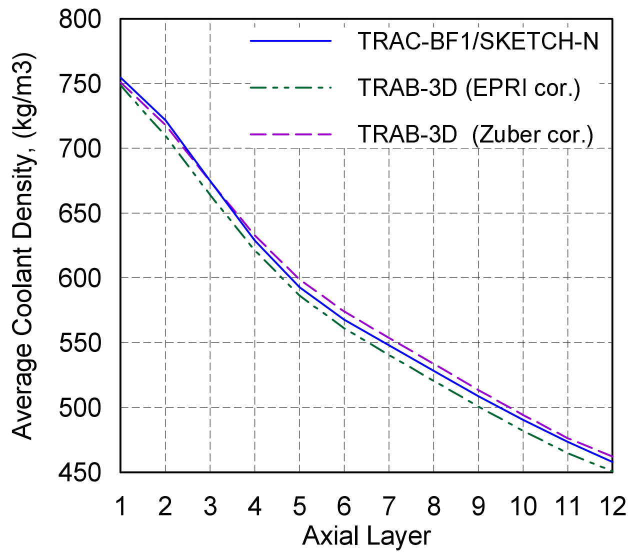

Figure 4 Axial distribution of coolant density.

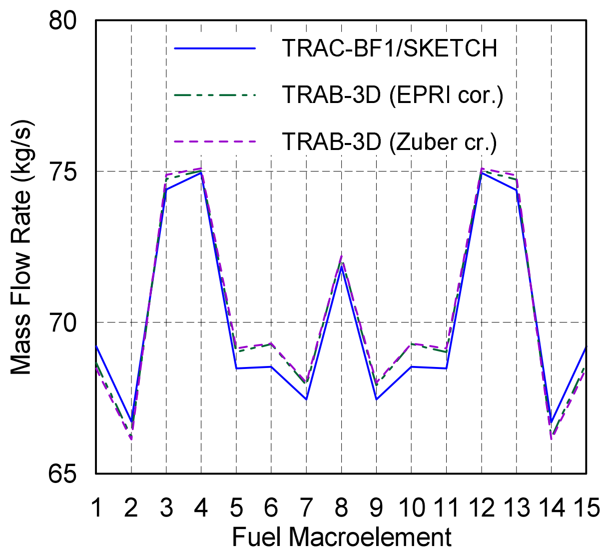

Figure 5. Mass flow rate along vertical traverse.

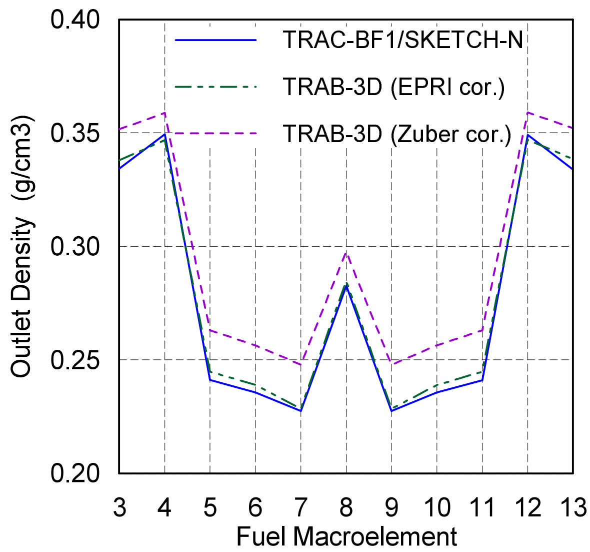

Figure 6. Channel outlet density along vertical traverse.

TRAB-3D (EPRI correlations)
TRAC-BF1/SKETCH
DIF(%)

	1	2	3	4	5	6	7	8
1:					0.055	0.086	0.112	0.144
1:					0.056	0.086	0.108	0.140
1:					-1.2	1.1	2.9	2.5
2:				0.125	0.290	0.424	0.457	0.635
2:				0.121	0.285	0.415	0.451	0.614
2:				3.6	1.9	2.1	1.2	3.3
3:			0.142	0.407	0.991	1.214	1.232	1.184
3:			0.139	0.406	0.977	1.202	1.222	1.169
3:			1.9	0.4	1.4	1.0	0.9	1.3
4:		0.128	0.418	1.026	1.511	1.558	1.577	1.145
4:		0.124	0.416	1.020	1.509	1.566	1.570	1.144
4:		3.6	0.3	0.6	0.1	-0.5	0.5	0.1
5:	0.062	0.294	0.996	1.513	1.753	1.731	1.836	1.780
5:	0.062	0.288	0.982	1.511	1.762	1.732	1.853	1.787
5:	-0.5	1.9	1.4	0.1	-0.5	0.0	-1.0	-0.4
6:	0.095	0.427	1.217	1.560	1.731	1.325	1.854	1.851
6:	0.094	0.418	1.205	1.568	1.732	1.332	1.869	1.883
6:	1.4	2.0	1.0	-0.5	-0.1	-0.5	-0.8	-1.7
7:	0.123	0.460	1.235	1.579	1.836	1.854	1.983	1.933
7:	0.119	0.455	1.224	1.571	1.854	1.870	2.017	1.957
7:	3.1	1.1	0.9	0.5	-1.0	-0.8	-1.7	-1.2
8:	0.157	0.639	1.186	1.146	1.780	1.851	1.933	1.496
8:	0.153	0.618	1.171	1.145	1.788	1.883	1.957	1.518
8:	2.7	3.3	1.3	0.1	-0.4	-1.7	-1.2	-1.5

Max. difference in 2D power distribution = 3.65% Location (x,y): (2,12)
Average difference in 2D power distribution = 1.24%
2D Power Peaking Factor (SKETCH-N) 2.0170 Location (x,y): (7,7)
2D Power Peaking Factor (TRAB-3D) 1.9827 Location (x,y): (7,7)
Difference in 2D Power Peaking Factors: -1.70%

Figure 7. A comparison of the TRAC-BF1/SKETCH-N and TRAB-3D (EPRI correlation) 2D power distributions.

5.3 Transient Results

Table 3 gives a summary of the TRAC-BF1/SKETCH-N and TRAB-3D transient results. As in the benchmark report (Finnemann et al., 1993), the values are given as differences with respect to the steady-state results. Generally there is a reasonable agreement between the codes. In contrast to the steady-state results, there is no clear correlation between a choice of the slip correlation in the TRAB-3D code and differences with the TRAC-BF1/SKETCH-N results. Anyway, the deviations between the results are rather small. In the following graphs, only results of the TRAB-3D code computed with the EPRI correlation are given. Fig. 8 shows the reactor power versus time. In this figure, we can see a time delay in the power increase computed by the TRAC-BF1/SKETCH code comparing with the TRAB-3D results. This time delay is attributed to the TRAC-BF1 reactor model shown in Fig. 1. In the TRAC model, cold water is injected using the `FILL` component; as a result there is small time delay in the perturbation because coolant has to pass through the inlet `PIPE` and lower plenum before reaching the `CHANNEL` inlet. Changes of the core-averaged Doppler fuel temperatures are compared in Fig. 9.

Table 3. Summary of the transient results of the NEACRP BWR cold water injection benchmark.

Parameter	TRAC-BF1/ SKETCH-N	TRAB-3D	
		EPRI Slip Correlation	Zuber-Findley Correlation
Maximum reactor power (%)	171.9	168.4 *-2.0 %*	167.2 *-2.7 %*
Time of maximum power, (s)	1.69	1.68 *-0.01 s*	1.79 *+0.1 s*
Difference in 3D power peaking factor at time of power peak vs. steady-state value (%)	11.5	10.4 *-1.1*	11.8 *+0.03*
Reactor power at the time 20 s, (%)	125.9	126.3 *+0.4*	126.1 *+0.2*
Difference in 3D power peaking factor at the time 20 s vs. steady-state value (%)	11.7	10.9 *-0.8*	11.0 *-0.7*
Difference in reactor average Doppler fuel temp. at time 20 s vs. steady-state value, (Δ°C)	64	68 *+4 ℃*	67 *+3 ℃*
Difference in maximum Doppler fuel temp. at the time 20 s vs. steady-state value, (Δ°C)	327	307 *-20 ℃*	324 *-3 ℃*
Difference in maximum centerline fuel temp. at time 20 s vs. steady-state value, (Δ°C)	793	694 *-99 ℃*	751 *-42 ℃*
Difference in outlet coolant temp. at time 20 s vs. steady-state value, (Δ°C)	-2.3	-2.1 *-0.2 ℃*	-2.2 *-0.1 ℃*
Difference in outlet coolant density at the time 20 s vs. steady-state value, ($\Delta kg/m^3$)	20.7	17.6 *-3.1* kg/m^3	17.9 *-2.8* kg/m^3
Difference in outlet void fraction at the time 20 s vs. steady-state value	-0.025	-0.022 *-0.003*	-0.022 *-0.003*

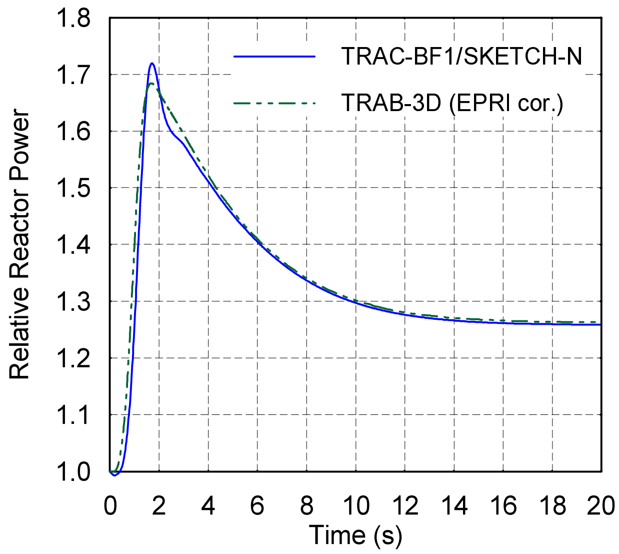

Figure 8. Relative reactor power versus time.

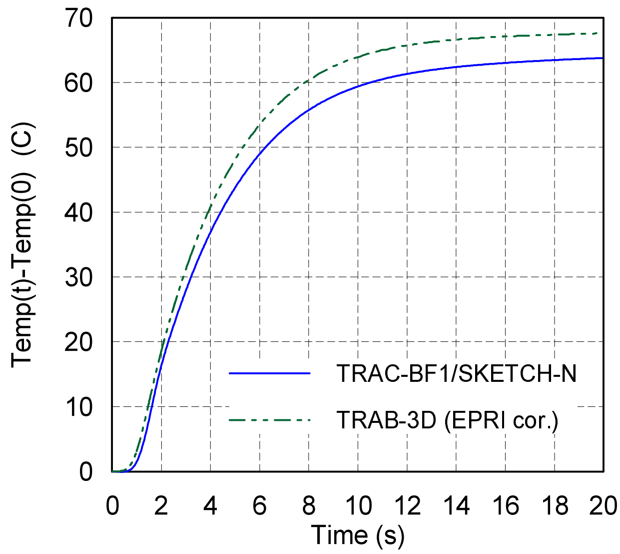

Figure 9. Change in core-averaged Doppler fuel temperature with respect to the steady-state value versus time.

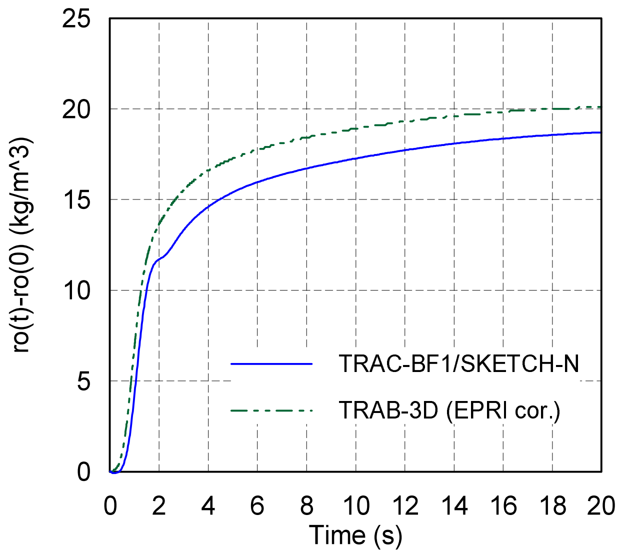

Figure 10. Change in core-averaged coolant density with respect to the steady-state value versus time.

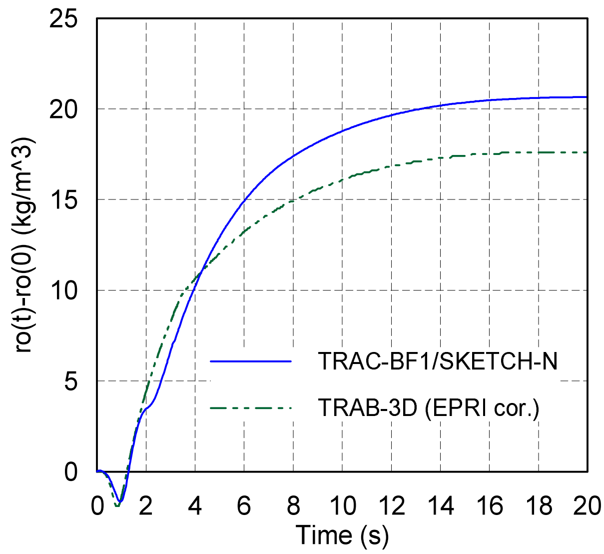

Figure 11. Change in core-averaged outlet coolant density with respect to the steady-state value versus time.

Fig. 10 and 11 show changes of the core-averaged and channel-outlet coolant densities versus time. The TRAC-BF1/SKETCH-N and TRAB-3D results are very close up to the time of the power peak. After this time moment, the TRAC results show slightly different trends, which are attributed to the TRAC thermal-hydraulics model. Fig. 12 shows changes in 3D power peaking factors versus time. Both the codes give very similar results. The change of the power shape is relatively small in this transient; maximum change in 3D power peaking factor is about 20 %. This is mostly due to the change of the axial power shape as illustrated in Fig. 13, where the changes of 1D, 2D and 3D peaking factors are shown versus time. The axial 1D and the 3D power peaking factors vary in the same way, while 2D radial power peaking factor changes less than 5 %. The results outline a main axial effect of this transient.

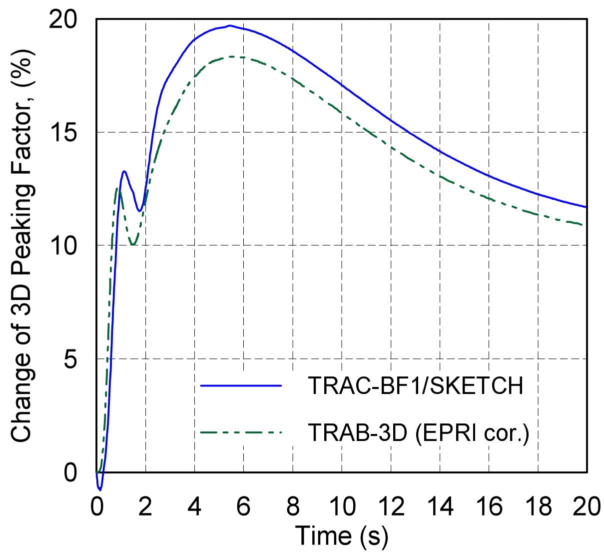

Figure 12. Change in 3D power peaking factors with respect to the steady-state value versus time

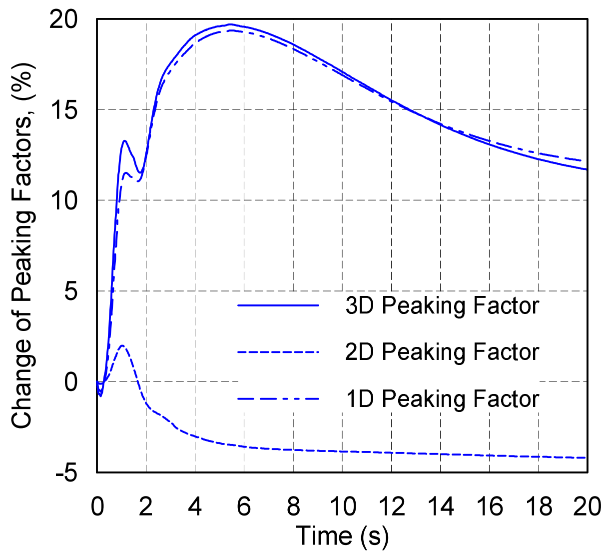

Figure 13. Change in 3D, 2D and 1D power peaking factors with respect to the steady-state value versus time; TRAC-BF1/SKETCH-N results.

6 Conclusions

NEACRP BWR cold water injection benchmark has been analyzed by two codes: TRAC-BF1/SKETCH-N code system by JAERI, Japan and TRAB-3D code by VTT Energy, Finland. Main features of the codes are given. Neutronics modules of both the codes are based on nodal methods. The TRAC-BF1 code uses two-phase two-fluid model of fluid dynamics, while TRAB-3D code applies the drift-flux formulation with four equations. TRAB-3D calculations are performed with two optional slip correlations: EPRI and Zuber-Findley.

Neutronics modules of the codes are separately estimated comparing the steady-state results computed with the same thermal-hydraulics data generated by the TRAB-3D code. SKETCH-N calculations are performed using two spatial meshes: the mesh used in the benchmark analysis and the mesh with a half mesh size. All the compared TRAB-3D and SKETCH-N results are in excellent agreement. The differences in power peaking factors are below 2 %; the maximum difference in eigenvalue is 52 pcm.

A comparison of the steady-state benchmark results also shows a close agreement, especially between the TRAC-BF1/SKETCH-N results and TRAB-3D results computed with the more advanced EPRI correlation. The difference in multiplication factors is 130 pcm, power peaking factors differ by 3.4 % and the difference in maximum fuel centerline temperatures is about 30 ºC. The two sets of the TRAB-3D results outline an effect of the slip correlation on the computed reactor parameters the most important being the effect on the axial power distribution. Change of the slip model results in 5 % change in 3D and 1D power peaking factors and 100 ºC change of the maximum fuel centerline temperature. The slip model has practically no effect on the radial power distribution, mass flow rate distribution and reactor-averaged Doppler fuel temperature.

A comparison of the transient results also shows reasonable agreement. In contrast to the steady-state results, there is no correlation between the slip model in TRAB-3D and the discrepancies between the TRAB-3D and TRAC-BF1/SKETCH-N results. However, the differences between the results are rather small. The values of power peak vary within 3 %; times of the power peak differ in 0.1 s. Several reactor parameters are compared at the time 20 s, when new steady-state condition is almost reached. The values of the reactor power differ within 0.5 %, the changes of the reactor-averaged Doppler fuel temperature with respect to the steady-state value differ within 5 ºC and the changes of the maximum fuel centerline temperature with respect to the steady-state value vary within 100 ºC. The plots of the reactor power peaking factors versus time show a main axial effect of the change of the power distribution, 2D power peaking factor changes less than 5 %. In our opinion, the reasonable results of this problem could be obtained with 1D neutron kinetics. However, an application of 1D neutron kinetics model requires consistent generation of 1D macro cross sections. Such option is not available presently in the SKETCH-N and TRAB-3D codes, leaving us a room for future extending of the code capabilities.

The authors will continue verification of the codes, especially in the area of fluid dynamics. An assessment of the TRAC-BF1/SKETCH-N code for BWR stability analysis is on the way using the OECD NEA Ringhals-1 stability benchmark. TRAB-3D has recently been validated against real BWR plant transients of the Finnish Olkiluoto 1 reactor (Daavittila et al., 2000). Calculation results for an overpressurization transient and an oscillation incident agreed well with measured data. Further participation in the OECD NEA benchmark calculations has also been planned.

Acknowledgments

The authors of JAERI are grateful to Mr. M. Enomoto and Miss M. Kano, both of Information Technologies of Japan (ITJ), Inc. for their help with the TRAC-BF1 code and to Dr. M. Hirano of JAERI for stimulating discussions.

References

Akimoto, H., et al., (1989). 18th Report on the Best-Estimate Code Development. J-TRAC User Manual (Version 62.1), JAERI-Memo-63-478, January 1989, *[In Japanese]*.

Asaka H., V.G. Zimin, T. Iguchi and Y. Anoda, (2000). Coupling of the Thermal-Hydraulics TRAC Codes with 3D Neutron Kinetics Code SKETCH-N. *Preliminary Proc. of the OECD/CSNI Workshop on Advanced Thermal-Hydraulic and Neutronics Codes: Current and Future Applications,* Barcelona, Spain, 10-13 April, 2000, vol. 2, pp. 1-15.

Borkowski, J. A., et al., (1992). TRAC-BF1/MOD1: An Advanced Best-Estimate Computer Program for BWR Accident Analysis. Model Description. NUREG/CR-4356, EGG-2626, Vol. 1, August 1992.

Chexal, B., and G. Lellouche, (1986). A Full-Range Drift-Flux Correlation for Vertical Flows (Revision 1). EPRI NP-3989-SR, Revision 1. Special Report, September 1986.

Daavittila, A., E. Kaloinen, R. Kyrki-Rajamäki, and H. Räty, (2000). Validation of TRAB-3D against Real BWR Plant Transients, to be Presented in *International Meeting on "Best-Estimate" Methods in Nuclear Installation Safety Analysis (BE-2000)*. Washington DC, November 2000.

Finnemann, H., and A. Galati, (1992). NEACRP 3-D LWR Core Transient Benchmark. Final Specifications, NEACRP-L-335 (Revision 1), January 1992.

Finnemann, H., H. Bauer, A. Galati, and R. Martinelli, (1993). Results of LWR Core Transient Benchmarks, NEA/NSC/DOC(93)25, October 1993.

Holt, R., and J. Rasmussen, (1972). RAMONA II, A Fortran Code for Transient Analysis of Boiling Water Reactors. Kjeller Report KR-147, Kjeller, Norway, 1972.

Kaloinen, E., and R. Kyrki-Rajamäki, (1997). TRAB-3D, a New Code for Three-Dimensional Reactor Dynamics, *Proc. of 5th International Conference on Nuclear Engineering ICONE-5,* CD-ROM, Paper ICONE5-2197, May 26-30, 1997, Nice, France.

Kaloinen, E., R. Kyrki-Rajamäki, and H. Räty, (1998). Calculation of BWR Transients with 3D Dynamics Code TRAB-3D. *Proc. of the Int. Conf. on the Physics of Nuclear Science and Technology (PHYSOR)*, October 5-8, 1998, Long Island, New York, American Nuclear Society, vol. 2, pp. 1444-1451.

Kaloinen, E., P. Siltanen, and R. Teräsvirta, (1980). Two-Group Nodal Calculation in Hexagonal Fuel Assembly Geometry. *Proc. of a Specialists' Meeting on the Calculation of 3-dimensional Rating Distributions in Operating Reactors*, OECD publications, Paris 1980, pp. 111-128.

Kyrki-Rajamäki, R., (1995). Three-Dimensional Reactor Dynamics Code for VVER Type Nuclear Reactors. VTT Publications 246, Espoo, Finland 1995.

Rajamäki, M., (1980). TRAB, a Transient Analysis Program for BWR, Part 1. Principles, Report 45. Technical Research Centre of Finland (VTT), Nuclear Engineering Laboratory, Helsinki, Finland 1980.

Sartori E. (1992). Corrections to the Specification – NEACRP-L-335. Letter to Participants in the 3D LWR Core Transient Benchmark, NDB/92/0385/avt, 27 March 1992.

Zimin, V.G., and H. Ninokata, (1998). Nodal Neutron Kinetics Model Based on Nonlinear Iteration Procedure for LWR Analysis. *Ann. Nucl. Energy,* **25**, 507-528.

Zimin, V.G., H. Ninokata, and L. Pogosbekyan, (1998). Polynomial and Semi-Analytic Nodal Methods for Nonlinear Iteration Procedure. *Proc. of the Int. Conf. on the Physics of Nuclear Science and Technology (PHYSOR)*, October 5-8, 1998, Long Island, New York, American Nuclear Society, vol. 2, pp. 994-1002.

Zimin, V.G., H. Asaka, Y. Anoda and M. Enomoto, (1999). Verification of the J-TRAC code with 3D Neutron Kinetics Model SKETCH-N for PWR Rod Ejection Analysis. *Proc. of the 9 International Topical Meeting on Nuclear Reactor Thermal Hydraulics (NURETH-9),* San Francisco, California, October 3-8, CD-ROM, 1999.

Zimin, V.G. (2000). SKETCH-N: A Nodal Neutron Diffusion Code for Solving Steady-State and Kinetics Problems, JAERI report, *[In preparation].*

Zuber, N., et al., (1967). Steady State and Transient Void Fraction in Two-Phase Flow Systems. Final Report for the Program of Two-Phase Flow Investigation. GEAP-5417, vol. 1., January 1967.